

**NASA Cooperative Agreement NCC 5 88
Chaos: Understanding and Controlling Laser Instability
University of Tennessee
P.I. William E. Blass**

Final Report - December 1997

Distribution:

Goddard Technical Officer: Dr. Gordon Chin, Code 693 -- 3 copies

NASA Scientific and Technical Information Facility,
Accessioning Dept., 800 Elkridge Road, Linthicum Heights, MD
21090 -- 2 copies

Ms. Gloria R. Blanchard, Code 286.1, Grants Officer -- 1 copy

Ms Dena Butler, Code 216 -- 1 copy

NASA Cooperative Agreement NCC 5 88
Chaos: Understanding and Controlling Laser Instability
University of Tennessee
P.I. William E. Blass

Final Report - December 1997
W. E. Blass and L. R. Senesac
Department of Physics and Astronomy

In order to characterize the behavior of tunable diode lasers (TDL), the first step in the project involved the redesign of the TDL system here at the University of Tennessee Molecular Systems Laboratory (UTMSL). Having made these changes it was next necessary to optimize the new optical system. This involved the fine adjustments to the optical components, particularly in the monochromator, to minimize the aberrations of coma and astigmatism and to assure that the energy from the beam is focused properly on the detector element. The next step involved the taking of preliminary data. We were then ready for the analysis of the preliminary data. This required the development of computer programs that use mathematical techniques to look for signatures of chaos. Commercial programs were also employed. We discovered some indication of high dimensional chaos, but were hampered by the low sample rate of 200 KSPS (kilosamples/sec) and even more by our sample size of 1024 (1K) data points.

These limitations were expected and we added a high speed data acquisition board. We incorporated into the system a computer with a 40 MSPS (million samples/sec) data acquisition board. This board can also capture 64K of data points so that we were then able to perform the more accurate tests for chaos. The results were dramatic and compelling -- we had demonstrated that the lead salt diode laser had a chaotic frequency output.

Having identified the chaotic character in our TDL data, we proceeded to stage two as outlined in our original proposal. This required the use of an Occasional Proportional Feedback (OPF) controller to facilitate the control and stabilization of the TDL system output. The controller was designed and fabricated at GSFC and debugged in our laboratories. After some trial and error efforts, we achieved chaos control of the frequency emissions of the laser.

The two publications appended to this introduction detail the entire project and its results.

Here we provide the references to the publications:

Stabilizing Lead-Salt Lasers: Understanding and Controlling Chaotic Frequency Emission, Gordon Chin, Larry R. Senesac, William E. Blass, and John J. Hillman, *Science* **274**, 1498-1501 (1996)

Stabilizing Lead-Salt Diode Lasers: Measuring and Controlling Chaotic Frequency Emission, Larry R. Senesac, William E. Blass, Gordon Chin, and John J. Hillman, *Proceedings of the 4th Experimental Chaos Conference*, August 1997, Boca Raton, FL, in press, World Scientific.

**Stabilizing Lead-Salt Diode Lasers:
Understanding and Controlling Chaotic
Frequency Emission**

Gordon Chin, Larry R. Senesac, William E. Blass,
and John J. Hillman

Stabilizing Lead-Salt Diode Lasers: Understanding and Controlling Chaotic Frequency Emission

Gordon Chin, Larry R. Senesac, William E. Blass,
John J. Hillman

Lead-salt tunable diode lasers (TDLs) are the only devices currently available that can generate tunable monochromatic radiation at arbitrary wavelengths between 3 and 30 micrometers and are particularly useful for high-resolution spectroscopy over a wide range of spectral regimes. Detailed observations of TDLs show that the observed instrumental linewidth is actually a temporal average of many narrow (less than 0.5 megahertz) emission "modes." The time scale characteristic of these "modes," which appear to be of relatively constant intensity, is of the order of a microsecond. The laser's behavior is highly suggestive of a chaotic process, that is, seemingly random excursions of a dynamic variable (frequency) within a bounded range. This report shows experimentally that TDL emissions are indeed chaotic. Furthermore, in a simple and robust fashion, this chaotic behavior has been successfully controlled with the use of recent techniques that take advantage of chaos to produce a narrow band laser output.

Chaotic behavior is an intrinsic property of a nonlinear system. Mechanical systems, communication and electronic systems, bio-

logical systems, the solar system, optical and laser systems, and many other nonlinear systems often exhibit chaotic behavior. Chaos is also often called deterministic random motion. The motion is deterministic because its trajectory can be calculated for all times given the starting conditions, but it is also motion in which instabilities appear everywhere in the system's trajectory in phase

G. Chin and J. J. Hillman, NASA Goddard Space Flight Center, Laboratory for Extraterrestrial Physics, Greenbelt, MD 20771, USA.

L. R. Senesac and W. E. Blass, Department of Physics and Astronomy, University of Tennessee, Knoxville, TN 37996-1200, USA.

space, the coordinate system describing a system's position and velocity. These instabilities force the trajectories of nearby phase-space points to diverge. This divergence is manifested as a sensitivity to initial conditions, another characteristic of chaotic motion. However, the nonlinearities of the system fold the trajectories back into a confined region. In this manner, chaotic motion amplifies small differences, errors, or noise, that is, the instabilities stretch phase space, whereas the nonlinearities, or folding motion, keep the trajectories bounded. Bounded trajectories signal the presence of an attractor. Another indication of chaotic behavior is the existence of a "strange" attractor with its distinctive fractal character. It is this fractal characteristic that gives chaotic motion its random appearance.

More recently, investigations of nonlinear dynamics have moved from purely theoretical and computational studies to experiment. Some of these experiments show that chaotic behavior is a useful feature in itself and more importantly may be exploited to perform practical functions (1). Following theoretical studies that reveal methods that stabilize unstable orbits (2, 3), a set of striking experiments ensued that demonstrated that chaos can be controlled in a surprisingly simple manner (4, 5) and in as diverse a range of problems as cardiac arrhythmia (6), thermal convection loops (5), electronic circuitry (7), an optical system (8), and solid-state lasers (9).

The practical demonstration of chaos control led us to consider whether these techniques are applicable to tunable diode lasers (TDLs). Lead-salt TDLs are valuable tools that are used to measure the molecular parameters of atmospheric constituents important in planetary atmospheres (10). The advantages of TDLs are wide spectral coverage (3 to 30 μm), achieved by varying the salt composition of an epitaxially grown lead-salt crystal (such as $\text{Pb}_{1-x}\text{Sn}_x\text{Te}$ or $\text{PbS}_{1-x}\text{Se}_x$), and high spectral resolution ($\sim 10^{-4} \text{ cm}^{-1}$). The TDLs are operated below 100 K and are tuned by changing the temperature or injection current (which effectively causes a change in the temperature of the laser junction). The combination of wide spectral coverage, continuous tunability, high resolution, high output power, and ease of use makes TDLs ideal for the study of line positions, line strengths, and pressure broadening coefficients, especially of molecules with closely spaced spectral transitions.

Despite the extremely successful use of TDLs in laboratory spectroscopy, the full potential of the TDL has not been realized. Careful characterization of a TDL shows that the intrinsic linewidth of its emission is very narrow ($<0.5 \text{ MHz}$ or $\sim 10^{-5} \text{ cm}^{-1}$), a factor of 10 better than the instrumental

resolution achieved in laboratory applications. The observed instrumental linewidth is actually a temporal average of many narrow frequency emissions or "modes" (12, 11). These instantaneous modes, which are relatively constant in intensity, change on a time scale on the order of a microsecond. This behavior is a natural consequence of the intrinsically nonlinear operation of a laser junction, where many microscopic facets or lasing regions may exist. Minute changes in the junction—such as in temperature, dimension, or index of refraction—can quench one lasing mode while allowing another to reach threshold. The detailed dynamics of such a complicated system is probably not amenable to analytical description.

Fortunately, numerical methods exist that can identify the presence of chaotic behavior without requiring a detailed knowledge of the underlying dynamics. However, the challenge remains how to capture the trajectory of the TDL in which the dynamical variable, frequency, varies at a megahertz rate. This information is also critical in our goal to control the TDL's chaotic emission.

The solution is to construct a frequency-to-amplitude converter (F/A) with a fast response time. We use one of two approach-

es: either an absorption cell containing a gaseous molecular sample or a Fabry-Perot etalon is placed in the path of the TDL's beam. By adjusting the TDL to lase on the steep side of either the gas line or the Fabry-Perot fringe, changes in the TDL frequency are converted to changes in detected signal amplitude. The F/A we used was an absorption transition of ethylene (C_2H_4) near 1029 cm^{-1} (Fig. 1A). However, an etalon or any other gas line within the tuning range of the TDL can work just as well. The advantages of using a gas absorption line are minimal losses in photon flux compared with those for a high-finesse etalon and the ability to control the slope of the F/A conversion by varying the pressure in the absorption cell.

We looked for signatures of chaotic behavior with several numerical tools. We first examined the power spectrum (12). Periodic oscillations in the data would produce spikes in the power spectrum. The power spectrum from our data is very broad, indicating that the emissions are not purely periodic. The largest Lyapunov exponent—a measure of the rate at which trajectories initially close together in phase space diverge (12, 13)—is 0.235 ± 0.022 for the filtered data in Fig. 1A, and the values ranged from 0.269 ± 0.013 to 0.314 ± 0.011 in other measurements. Positive Lyapunov exponents characterize chaotic data, whereas periodic data have negative values. There are two tests that measure the dimension of the chaotic attractor in phase space: the capacity (or Hausdorff) dimension (12) and the correlation dimension (14). Both measures yield a dimension of about 4 for the raw TDL data (and about

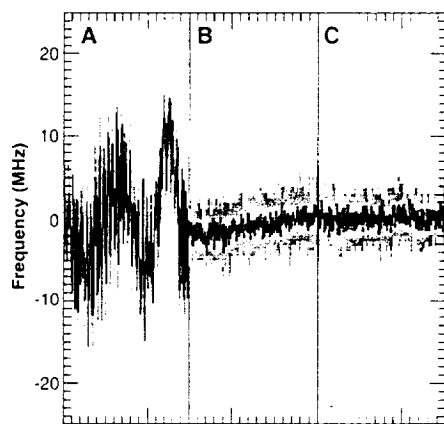


Fig. 1. The frequency variation of a lead-salt TDL operating near 1029 cm^{-1} using a line of ethylene as the F/A converter. Each panel has 30,000 points digitized with a 20-MHz 8-bit analog-to-digital converter. The colored points are the measured data. The black plot shows the results of applying a digit low-pass filter to the measurements. The frequency scale was calibrated with the use of methods similar to those used in (10, 11). (A) Chaotic TDL emission without control. (B) TDL emission with the OPF electronics on. (C) Detector noise level when the laser beam is blocked. The difference between the filtered and unfiltered data is identical to the noise, showing that we succeeded in taking out only the detector noise. The interval of the measurements was 1.5 ms; the data in the three panels were not taken contiguously.

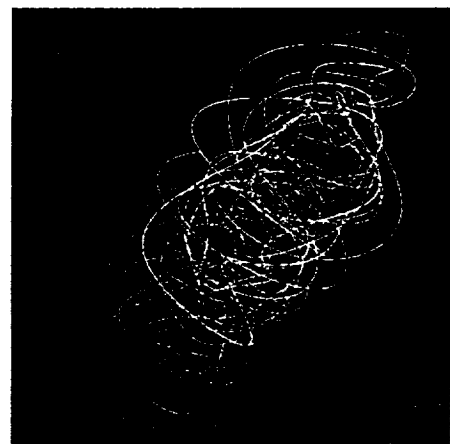


Fig. 2. A 3D time-delay phase plot of the TDL frequency trajectory, from the measurements displayed in Fig. 1A. The trajectory shows intricate spiral structure embedded within spiral structure. An animated version of this figure reveals stretching and folding motions. The points are colored to show the time evolution of the trajectory, from blue to red. The axes indicate frequency in megahertz.

A three-dimensional (3D) phase-space portrait (16) of the TDL filtered data using time-delay coordinates (Fig. 2) reveals a trajectory that is composed of strikingly complex embedded spirals. For stochastic data or random noise, such a plot shows no structure, and the trajectory randomly fills phase space. If the data are periodic, then the trajectory forms a closed orbit. An animated 3D phase portrait (17) shows the stretching and folding motions in the TDL frequency excursions. The TDL trajectory is confined, yet it never repeats—again a signature of chaos.

The block diagram illustrates the OPF controller system. It features a dashed-line boundary enclosing the main control logic. Outside this boundary, the 'Cryogenic temperature stabilizer' provides input to the 'Tunable diode laser'. The 'Laser current supply' also provides input to the 'Tunable diode laser'. The 'Tunable diode laser' is connected to the 'Etalon or gas cell'. The 'Etalon or gas cell' provides input to the 'Monochromator'. The 'Monochromator' provides input to the 'Detector and pre-amp'. The 'Detector and pre-amp' provides input to the 'Input gain' block. The 'Input gain' block provides input to the 'Offset adjust' block. The 'Offset adjust' block provides input to the 'Sample and hold' block. The 'Sample and hold' block provides input to the 'Window detector' block. The 'Window width' block provides input to the 'Window detector' block. The 'Window detector' block provides input to the 'Control logic' block. The 'Clock pulse' block provides input to the 'Control logic' block. The 'Control logic' block provides input to the 'Multiplexer' block. The 'Multiplexer' block provides input to the 'Output gain' block. The 'Output gain' block provides the final output. The 'OPF controller' label is positioned below the dashed-line boundary.

1500

Figure 1 consists of two panels, A and B. Panel A is a 2D frequency-frequency correlation spectrum. The x-axis is labeled 'Frequency (MHz)' and ranges from -20 to 20. The y-axis is also labeled 'Frequency (MHz)' and ranges from -20 to 20. The plot shows a dense collection of peaks, with a strong diagonal line of peaks and numerous off-diagonal cross-peaks, indicating correlations between different frequency components. Panel B is a 1D ^1H NMR spectrum. The x-axis is labeled 'Frequency (MHz)' and ranges from -20 to 20. The y-axis is labeled 'Relative number' and ranges from 0.0 to 1.0. The spectrum shows a sharp, prominent peak at 0 MHz, with a broad, low-intensity background signal across the rest of the frequency range.

SCIENCE • VOL. 274 • 29 NOVEMBER 1996

For our problem, we monitor the frequency excursion, with the F/A method described above, and use the injection current of the TDL as the accessible system parameter (Fig. 3). The output frequency of a TDL is coarse-tuned by the operating temperature in a close-cycle refrigerator and fine-tuned by the injection current. The F/A output, from a detector preamplifier, enters the OPF electronics through a variable-gain input. An offset is added to the input signal to center it in a window. This signal is fed to a window detector and a sample-and-hold amplifier. The F/A signal is checked to determine if it lies within the adjustable width of the window. If so, the sampled signal is fed through a variable-gain output amplifier as a correction to the TDL control module, which adds it to the TDL injection current. The sampling rate and output correction signal are synchronized by an external clock, in our case running at 1 MHz.

Our measurements are all dominated by detector noise (the colored plots in Fig. 1). Because it is primarily high frequency (Fig. 1C), we felt it appropriate to apply digital low-pass filtering to our data to improve our measurement accuracy. The amount of filtering was determined by the requirement to preserve the characteristic of the TDL chaotic emission without any distortion.

control was robust and continued indefinitely without further adjustment.

The slight drift in frequency in Fig. 1B is attributable to a small and slow 100-Hz ramp in the injection current from the TDL control module. This drift shows that OPF control can be maintained while varying the center frequency of the TDL. We achieved similar results with a fixed Fabry-Perot etalon as the F/A by tuning the TDL to one side of a low-finesse etalon fringe. We maintained OPF control while scanning the frequency over a range of ~ 80 MHz. This range is of practical importance as it demonstrates that OPF can be used with a TDL to scan across a molecular absorption feature and to perform spectroscopic measurements at higher frequency resolution than previously possible.

We can only give an upper limit to the frequency stability attained with the OPF method because the measurements are dominated by detector noise that can only be improved by signal processing (Fig. 1). Another factor is that our F/A process inseparably convolves amplitude and frequency variations. To calculate an upper limit, we project the trajectories in two dimensions (Fig. 4A). A histogram of the number of points in each 0.2-MHz bin of the controlled and uncontrolled emission is then made (Fig. 4B). From a Gaussian fit to the controlled distribution, we obtain a value for its full width at half maximum (FWHM), here being 1.68 MHz, which we can use as a strict upper limit.

An equal partitioning of the intensity and frequency variations in quadrature, a reasonable assumption, would reduce the frequency limit by $\sqrt{2}$, to 1.19 MHz. The FWHM of the uncontrolled TDL excursion, measured by hand, is ~ 18 MHz. Therefore, the OPF method improves the TDL frequency stability by at least a factor of 11 to 15. We can determine more accurately the frequency stability by heterodyning the TDL output with a stabilized 10- μm CO_2 laser.

The improved stability, in both the frequency and the amplitude of the OPF-controlled TDL, will enable new applications. We have mentioned higher resolution spectroscopy that scans a TDL. An OPF-controlled TDL can also be used as a local oscillator for heterodyne radiometers. The far-infrared (FIR) spectral regime is extremely important, and the recent development of wide-bandwidth hot-electron bolometer mixers makes the need for a suitable FIR local oscillator immediate. There are numerous candidates for future OPF control, such as an optically pumped sub-millimeter laser that emits from 30 μm to 1 mm and whose output varies in a seemingly random fashion because of nonlinear feedback between the pump and lasing gas.

REFERENCES AND NOTES

1. "Chaos in Communications," *Proc. SPIE* 2038 (1993).
2. E. Ott, C. Grebogi, J. A. Yorke, *Phys. Rev. Lett.* **64**, 1196 (1990).
3. U. Dressler and G. Nitsche, *ibid.* **68**, 1 (1992); F. Romeiras, C. Grebogi, E. Ott, W. P. Dayawansa, *Physica D* **58**, 165 (1992); H. Wang and E. H. Abed, *Proceedings of IFAC Nonlinear Control Systems Symposium, Bordeaux* (1992).
4. W. L. Ditto, S. N. Rauser, M. L. Spano, *Phys. Rev. Lett.* **65**, 3211 (1990).
5. J. Singer, Y.-Z. Wang, H. H. Bau, *ibid.* **66**, 1123 (1991).
6. A. Garinkel, M. L. Spano, W. L. Ditto, J. N. Weiss, *Science* **257**, 1230 (1992).
7. E. R. Hunt, *Phys. Rev. Lett.* **67**, 1953 (1991).
8. T. Takizawa, Y. Liu, J. Ohtsubo, *IEEE J. Quantum Electron.* **30**, 334 (1994).
9. R. Roy, T. W. Murphy Jr., T. D. Maier, Z. Gills, E. R. Hunt, *Phys. Rev. Lett.* **68**, 1259 (1992); Z. Gills, C. Iwata, R. Roy, I. B. Schwartz, I. Triandaf, *ibid.* **69**, 3169 (1992).
10. D. E. Jennings, *J. Quant. Spectrosc. Radiat. Transfer* **40**, 221 (1988).
11. ———, *Appl. Opt.* **23**, 1233 (1984).
12. J. P. Eckmann and D. Ruelle, *Rev. Mod. Phys.* **57**, 617 (1985).
13. J. P. Eckmann, S. O. Kamphorst, D. Ruelle, S. Ciliberto, *Phys. Rev. A* **34**, 4971 (1986).
14. M. Ding, C. Grebogi, E. Ott, T. Sauer, J. A. Yorke, *Phys. Rev. Lett.* **70**, 3872 (1993).
15. D. S. Broomhead and G. P. King, *Physica D* **20**, 217 (1986).
16. N. H. Packard, J. P. Crutchfield, J. D. Farmer, R. S. Shaw, *Phys. Rev. Lett.* **45**, 712 (1980).
17. An animated phase portrait of one of our data sets can be viewed on our World Wide Web site at <http://aurora.phys.utk.edu/~senesac/>.
18. T. W. Carr and I. B. Schwartz, *Phys. Rev. E* **51**, 5109 (1995); *Physica D*, in press.
19. We thank J. Lobell for designing the OPF electronics and G. Miller for putting it together [they are in Code 692 of the Goddard Space Flight Center (GSFC)]. M. Sirota and D. Reuter (Code 693) loaned us the diode laser for this experiment. This research was conducted under NASA cooperative agreement NCC 5-88 with the University of Tennessee under the support of the GSFC Director's Discretionary Fund.

29 July 1996; accepted 23 September 1996

STABILIZING LEAD-SALT DIODE LASERS: MEASURING AND CONTROLLING CHAOTIC FREQUENCY EMISSION

LARRY R. SENESAC and WILLIAM E. BLASS

*Department of Physics and Astronomy, The University of Tennessee
Knoxville, TN 37996-1200, USA*

and

GORDON CHIN and JOHN J. HILLMAN

*NASA Goddard Space Flight Center, Laboratory for Extraterrestrial Physics
Greenbelt, MD 20771, USA*

ABSTRACT

Close observations of the emission from a lead-salt tunable diode laser (TDL) reveal that the observed instrumental linewidth is actually a temporal average of many narrow (less than 0.5 megahertz) emission "modes." Though the instantaneous laser output width is less than 0.5 MHz, the working width of the laser is limited to several MHz by frequency jitter. Since the jitter frequency is a dynamic system variable which occurs within a bounded range but varies in what appears to be a random fashion, chaotic behavior is suggested. With this in mind we designed a procedure to monitor and measure these frequency fluctuations on our own lead-salt TDL system. We then analyzed the data and discovered that the fluctuations are indeed indicative of a chaotic process. Utilizing the chaos control technique of occasional proportional feedback (OPF) developed in 1991 by E. R. Hunt, we constructed an electronic OPF controller. With this controller we succeeded in decreasing the frequency variations by at least a factor of twenty over the same laser emission without the controller.

1. Introduction

In the 1990s, investigations of nonlinear dynamics have moved from purely theoretical and computational studies to experiment. Some of these experiments show that chaotic behavior is a useful feature in itself and more importantly may be exploited to perform practical functions¹. Following theoretical studies that reveal methods that stabilize unstable orbits^{2,3} a set of striking experiments ensued that demonstrated that chaos can be controlled in a surprisingly simple manner^{4,5} and in as diverse a range of problems as cardiac arrhythmia⁶, thermal convection loops⁵, electronic circuitry⁷, an optical system⁸, and solid-state lasers^{9,10}. We report here on new data and new results which validate and extend the work first reported in 1996¹³.

The practical demonstration of chaos control led us to consider whether these techniques are applicable to tunable diode lasers (TDLs). Lead-salt TDLs are valuable tools for the study of molecular parameters of atmospheric constituents important in planetary atmospheres¹¹. TDLs are operated at temperatures below 100 K and their frequency output is tuned by changing the diode temperature or injection current (which effectively causes a change in the temperature of the laser junction).

Despite the extremely successful use of TDLs for laboratory spectroscopy, the full potential of a TDL has not been realized. Careful characterization of a TDL shows that the intrinsic linewidth of its emission is very narrow (< 0.5 MHz or $\sim 10^{-5}$ cm⁻¹), a factor of 10 better than the instrumental resolution achieved in laboratory applications. The observed instrumental linewidth is actually a temporal average of many narrow frequency emissions or "modes"^{11,12}. These instantaneous modes, which are relatively constant in intensity, change on a time scale on the order of a microsecond. This behavior is a natural consequence of the intrinsically nonlinear operation of a laser junction where potentially many microscopic facets or lasing regions exist. Minute changes in the junction - such as in temperature, dimension, or index of refraction - can quench one lasing mode while allowing another to reach threshold. Though the instantaneous laser output width has been determined to be less than 0.5 MHz, the working width of the laser is limited to several MHz¹² by frequency jitter resulting from this nonlinear operation. Since the jitter frequency is a dynamic system variable which occurs within a bounded range but varies in what appears to be a random fashion, chaotic behavior is suggested. The detailed dynamics of such a complicated system is probably not amenable to analytical description.

2. Frequency To Amplitude Converter - F/A

Our first challenge is to capture the frequency fluctuation information from the TDL emission. Our solution is to construct a frequency-to-amplitude converter (F/A) with a fast response time. We use one of two approaches: either an absorption cell containing a gaseous molecular sample or a Fabry-Perot etalon is placed in the path of the TDL's beam. By adjusting the TDL to lase on the steep side of either the gas line or Fabry-Perot fringe, changes in the TDL frequency are converted to changes in detected signal amplitude. In Figure 1 we see an illustration of this technique. The region on the side of an interferometer fringe, or a molecular absorption line, looks approximately linear and has a fairly steep slope. For the sake of clarity in the figure, we show only the center portion of the side of the line, scaled for our convenience. We begin by tuning the laser frequency so that it is on the center of the side of the line. We then note the amplitude of the signal there (marked as Center Line in the figure). If the frequency of the laser decreases, as at point A, we immediately detect a decrease in the amplitude of the signal. Similarly, if there is a decrease in the laser frequency as at point B, we detect a decrease in signal ampli-

tude. Having previously described the use of an absorption line F/A^{13} , in this paper we will examine the results of using an etalon fringe F/A .

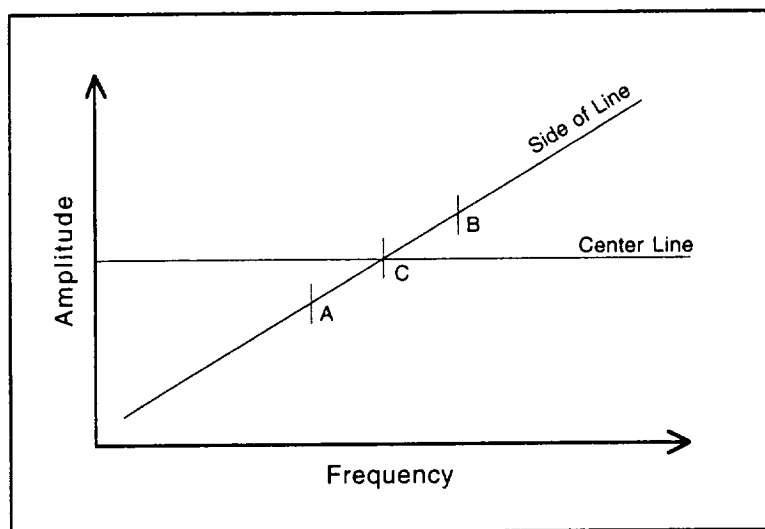


FIGURE 1 Frequency to Amplitude conversion. Shown is the side of an absorption line or etalon fringe. We tune the frequency so that it is at the center of the side at point C and hold the frequency there. If the frequency of the laser decreases, as at point A, we immediately see a decrease in the amplitude of the signal. If the frequency increases, as at point B, we see an increase in amplitude.

3. Examining The Frequency Fluctuations For Chaotic Character

The F/A utilized in this investigation is a 3" solid Germanium etalon, and we were operating the TDL at 1029 cm^{-1} . In Figure 2 is plotted the frequency variation of the TDL emission. In (A) is plotted the raw data, and in (B) is plotted the same data filtered to remove noise. The data was taken with an 8-bit analog-to-digital converter, with a sampling rate of 500 kHz.

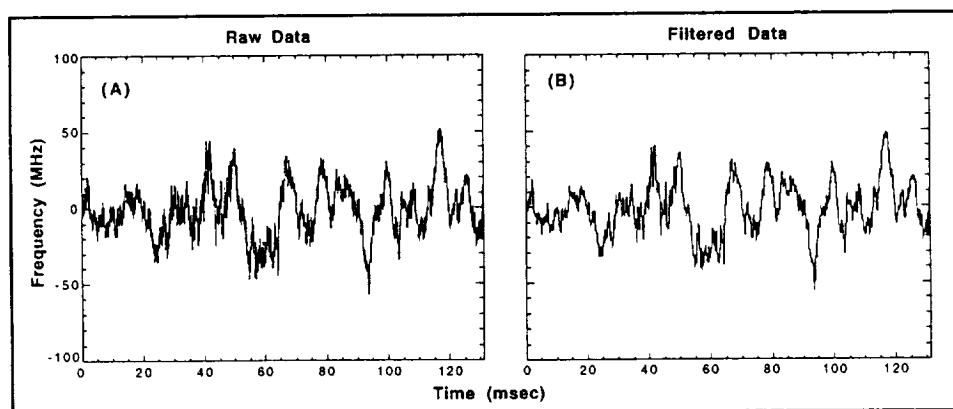


FIGURE 2 The frequency variation of a lead-salt TDL. In (A) is plotted the raw data, and in (B) is plotted the same data filtered to remove noise.

We looked for the signature of chaotic behavior with several numerical tools. The largest Lyapunov exponent¹⁴ was found to be 0.202 ± 0.055 for this data. The capacity dimension¹⁵ was calculated to be 1.205 ± 0.066 for the raw data, and 1.368 ± 0.075 for the filtered data. In Figure 3 is plotted the correlation dimension¹⁶ as a function of embedding dimension for the Raw and Filtered data. We see that in the raw data, the presence of experimental background noise makes the correlation difficult to calculate, and also yields an artificially high value for the dimension. The filtered data gives a smoother plot, and shows a plateau onset for the correlation dimension of 2.858 ± 0.272 .

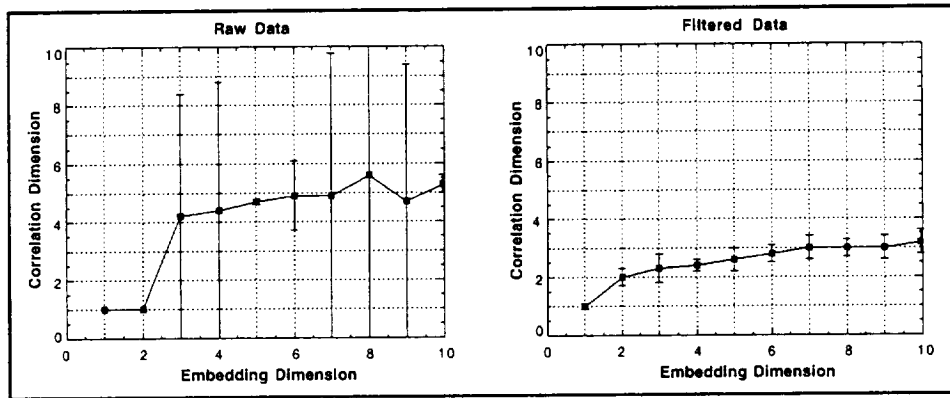


FIGURE 3 The Correlation dimension for the raw and filtered data.

Another indicator of chaotic character is the power spectrum¹⁵. In Figure 4 we have plotted the log of the power spectrum as a function of frequency for the raw data. The power spectrum of the filtered data looks nearly identical except that it is attenuated at high frequencies. We see that the data has a very broad power spectrum indicating that the laser emission is not purely periodic.

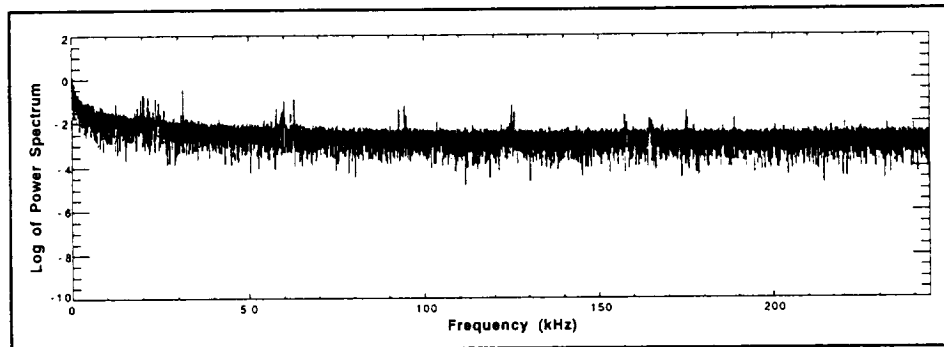


FIGURE 4 The Log of the Power Spectrum vs. frequency.

In Figure 5 we have used time-delay coordinate embedding¹⁷ to create a phase-space portrait of the filtered data. The plot uses only 10,000 of the 65,000

data points so that we may see the trajectory more clearly. The plot reveals a trajectory that is composed of strikingly complex embedded spirals. The trajectory is confined to a region of phase-space yet it never repeats. This is again indicative of a chaotic process. A phase plot of the entire data set may be seen in Figure 8 (A).

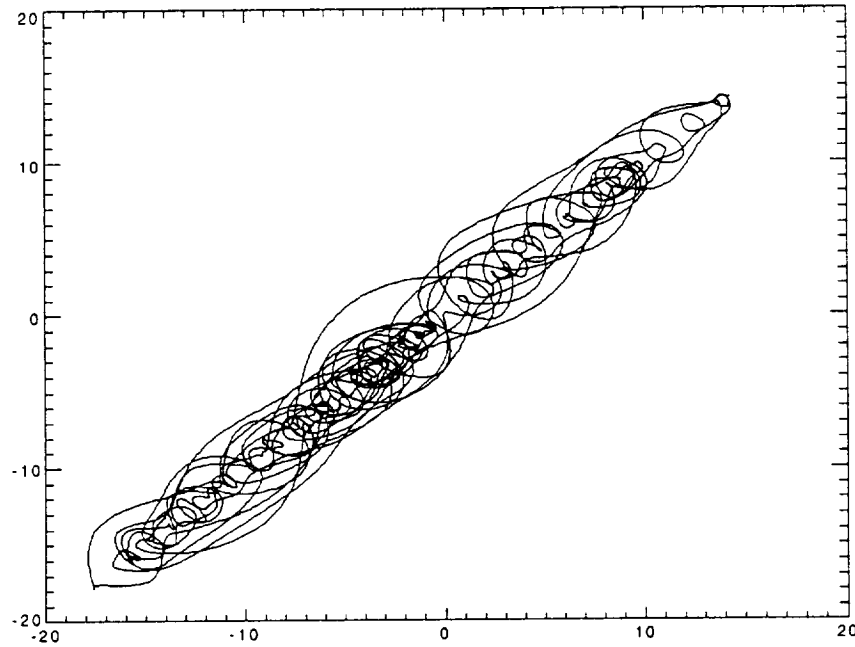


FIGURE 5 Time-delay coordinate phase-space portrait for the filtered data. The axes indicate frequency in MHz.

4. Control Of Chaos

Having established to our satisfaction that the TDL emission indicates a chaotic process, our next goal was the control of this chaotic behavior. In 1990 the first papers emerged which focused on the control of chaos in physical systems. The first paper published by Ott, Grebogi, and Yorke² set the stage for the chaos control papers which followed. The method outlined in the paper, referred to by most as the OGY method, was based on the idea that the chaotic attractor for the system is made up of an infinite number of unstable periodic orbits. The first step of the OGY method is to monitor one (or some) of the system variables, and use the delay-coordinate embedding technique¹⁷ to construct the chaotic attractor in the phase space of the system. Next, from this attractor find one of the orbits which yields the desired system behavior and locate the fixed points of that orbit. And finally a small time-dependent perturbation is made in an accessible system parameter to keep the fixed point in the path of the system trajectory. This forces the system to remain in the desired orbit. The idea is to take advantage of the system's sensitive dependence on initial conditions and use minor perturbations to the system to produce the desired behavior.

Closely following the OGY paper Ditto, Rauseo, and Spano⁴ used the OGY method to stabilize a physical chaotic two state system and switch between the two states at will. These papers were followed quickly by a plethora of chaos control studies in widely diverse areas from controlling the flow of water in a thermal convection loop⁵ to stabilizing cardiac arrhythmias⁶.

5. Occasional Proportional Feedback

In 1991 E. R. Hunt developed a modification of the OGY method which used occasional proportional feedback (OPF) to find, stabilize, and switch between nineteen different orbits from the chaotic attractor of a diode resonator⁷. One advantage of the OPF method is that we do not need a detailed knowledge of the dynamics of the system nor is it necessary to know initially where the fixed points of the system lie. In fact, the OPF method can be used to allow the system to find stable orbits by itself. The basic method of OPF is to sample an accessible dynamic system variable, and if the value of the variable falls within a prescribed range or "window", a system parameter is modulated with an amplitude proportional to the difference between the value of the sampled variable and the center of the window.

Another difference between the OPF method and the OGY method is that the perturbations made to the accessible system parameter, necessary to stabilize the orbit, are not restricted to being small in the OPF method. Hunt found that with large perturbations the attractor could be altered and periodic orbits could be found where none had existed previously. OPF has more recently been used to control a chaotic solid state laser system⁹ and also to synchronize a pair of diode resonators¹⁸. An explanation of why OPF works and an extension of this method using the duration of the feedback control as an additional control parameter that is effective for higher complexity systems is found in Carr and Schwartz¹⁹.

6. Our OPF Controller System

For our OPF controller, we monitor the frequency excursion of the laser output (with the F/A method described above) as our dynamic system variable, and use the injection current to the TDL as our accessible system parameter. In Figure 6 is a diagram for our OPF controller and TDL system. The output frequency of the TDL is coarse-tuned by the operating temperature in a close-cycle helium refrigerator and fine-tuned by the injection current. The F/A output, from a detector pre-amplifier, enters the OPF electronics through a variable-gain input. An offset is added to the input signal to center it in a window. This signal is fed to a window detector and a sample-and-hold amplifier. The F/A signal is checked to determine if it lies within the adjustable width of the window. If so, the sampled signal is fed through a variable-gain output amplifier as a correction to the laser current supply where it is added to the TDL injection current. The sampling rate of the OPF controller sample-

and-hold amplifier and the timing of the output correction signal are synchronized by an external clock, in our case running at 1 MHz.

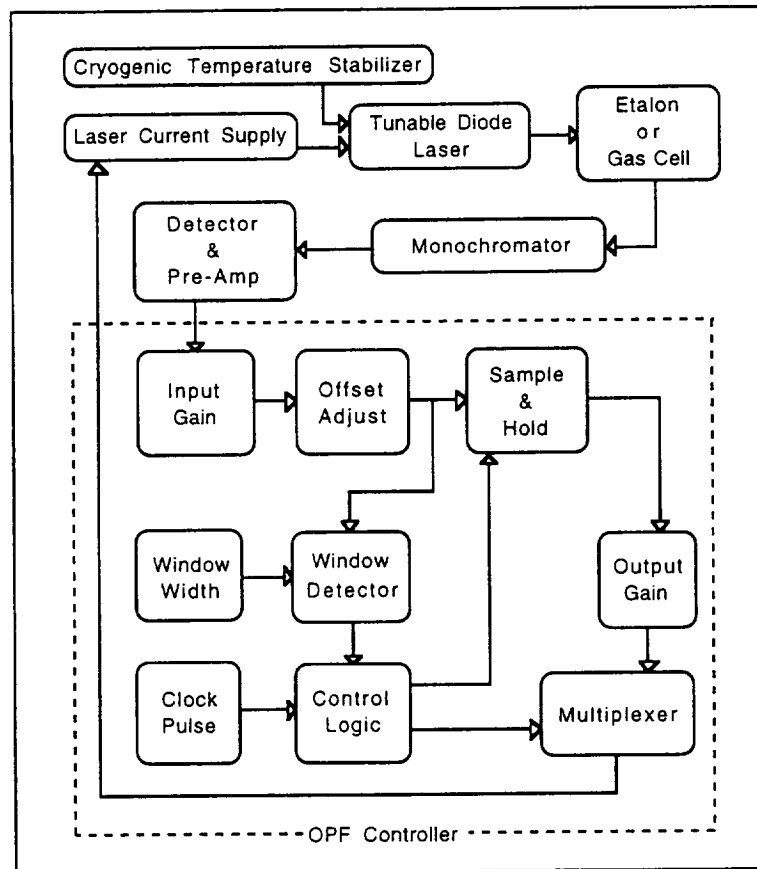


FIGURE 6 OPF controller and system diagram.

Several parameters determine how well the OPF method works. For example, TDL control is dependent on clock speed. For clock speeds slower than 600 kHz, OPF control diminishes. Otherwise the exact OPF clock speed is not critical and our experiments are all conducted at 1 MHz. The sensitivity of the F/A conversion is another important factor. High sensitivity in the F/A conversion, that is small values of $\Delta V/\Delta \nu$ (for voltage V and frequency ν), or the steepness of the line where the laser is tuned, causes difficulty in control¹³. The etalon fringe we used here has a 6.7 V/GHz slope (to convert from voltage variation to frequency, we used 150 MHz/V). This slope is much lower than the slope of the molecular absorption line used in previous experiments¹³, and the control is smoother. The width of the OPF window, on the other hand, is not a sensitive parameter. Once stable TDL emission was established, OPF control was robust and continued indefinitely without requiring any further adjustments.

7. Experimental Results

Figure 7 shows the results from one of our experiments. Control of the TDL emission was established quickly in a simple and robust fashion as the gain of the correction signal is gradually increased. The chaotic TDL emission (Fig. 7 A) can be contrasted to the stability acquired when OPF control is fully active (Fig. 7 B). (The uncontrolled data (A) is the same data as in Figure 2). The controlled TDL emission is stable in both frequency and amplitude.

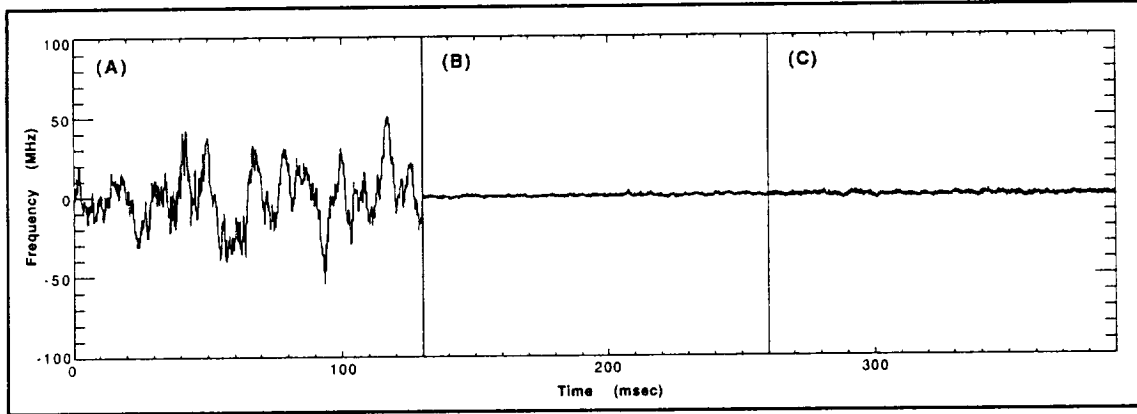


FIGURE 7 In (A) is plotted the chaotic uncontrolled TDL emission. In (B) is the TDL emission with the OPF controller on, and in (C) is the signal noise level with the TDL beam blocked. The data was filtered to remove the detector noise. The interval of each measurement was 130 msec, and the data in the three panels were not taken contiguously.

Figure 7 C shows the detector noise, here the TDL laser beam is blocked. Our measurements are all dominated by detector noise. Because the detector noise is primarily high frequency, we felt it appropriate to apply digital low-pass filtering to our data to improve our measurement accuracy. Therefore the data shown in Figure 7 shows the results of the filtering. (The raw uncontrolled emission can be seen in Figure 2.) The amount of filtering was determined by the requirement to preserve the characteristic of the TDL chaotic emission without any distortion.

We shall now compare the frequency fluctuations in the controlled versus the uncontrolled data. The total deviation for the uncontrolled laser emission is 109 MHz, with a standard deviation of 17.3 MHz for the unfiltered data, and 104 MHz, with a standard deviation of 17.2 MHz for the filtered data. We see that the filtering of the high frequency noise has very little effect on the uncontrolled laser emission (as can be seen visually in Figure 2).

For the controlled laser we find that the total deviation is 11.7 MHz, with a standard deviation of 1.45 MHz for the unfiltered data, and 5.57 MHz, with a standard deviation of 0.63 MHz for the filtered data. While the post-filtering of the data had very little effect on the uncontrolled laser emission, we see that the standard deviation of the controlled emission is reduced by over half, indicating that the controlled laser signal is background noise limited.

The filtered background signal noise has a total deviation of 11.7 MHz, with a standard deviation of 1.35 MHz for the unfiltered data, and 6.08 MHz, with a standard deviation of 0.83 MHz for the filtered data. The comparison of the above statistics for the controlled emission and the background detector noise again indicates that the controlled laser emission is background noise limited, and that our filtering is therefore justified. For the filtered data, the ratio of the standard deviations for the uncontrolled and controlled emission indicate a reduction in frequency fluctuation by a factor of 27.

8. Upper Limit To Frequency Stabilization

We can only give an upper limit to the frequency stability attained with the OPF method because the measurements are dominated by detector noise that can only be improved by signal processing. Another factor is that our F/A process inseparably convolves amplitude and frequency variations. To calculate an upper limit, in Figure 8 (A) we project the trajectories in two dimensions of the uncontrolled (black) and stabilized (small white region in center) laser emission. In Figure 8 (B) we have plotted the histograms for both the uncontrolled laser emission data (1), and the controlled emission data (2). The bin width for the histogram is 1 MHz. A Gaussian profile was then fitted to each histogram, and the profile was over-plotted onto the histogram. The Gaussian fitted to the uncontrolled laser data has a FWHM of 29.5 MHz, while the Gaussian fitted to the controlled laser data has a FWHM of 1.45 MHz. We may use this FWHM of 1.45 MHz as a strict upper limit. An equal partitioning of the intensity and frequency variations in quadrature, a reasonable assumption, would reduce the frequency limit by $\sqrt{2}$ or to 1.03 MHz. Since the FWHM of the uncontrolled TDL excursion was found above to be 29.5 MHz, we find that the OPF method improves the TDL frequency stability by at least a factor of 20 to 29.

9. Scanning The Center Frequency Of The Controlled TDL

In Figure 9 we have plotted the successful scan of the center frequency of the TDL with the OPF controller activated. The range of the scan is 120 MHz (4 mcm^{-1}). This is of practical importance as it demonstrates that OPF can be used with a TDL to scan across a molecular absorption feature and to perform spectroscopic measurements at higher frequency resolution than previously possible.

The improved stability, both in frequency and amplitude of the OPF-controlled TDL, will enable new applications. In addition to the high resolution spectroscopy mentioned above, an OPF-controlled TDL can also be used as a local oscillator (LO) for heterodyne radiometers. The far-infrared (FIR) spectral regime is extremely important and the recent development of wide-bandwidth hot-electron bolometer mixers makes the need for suitable FIR LO

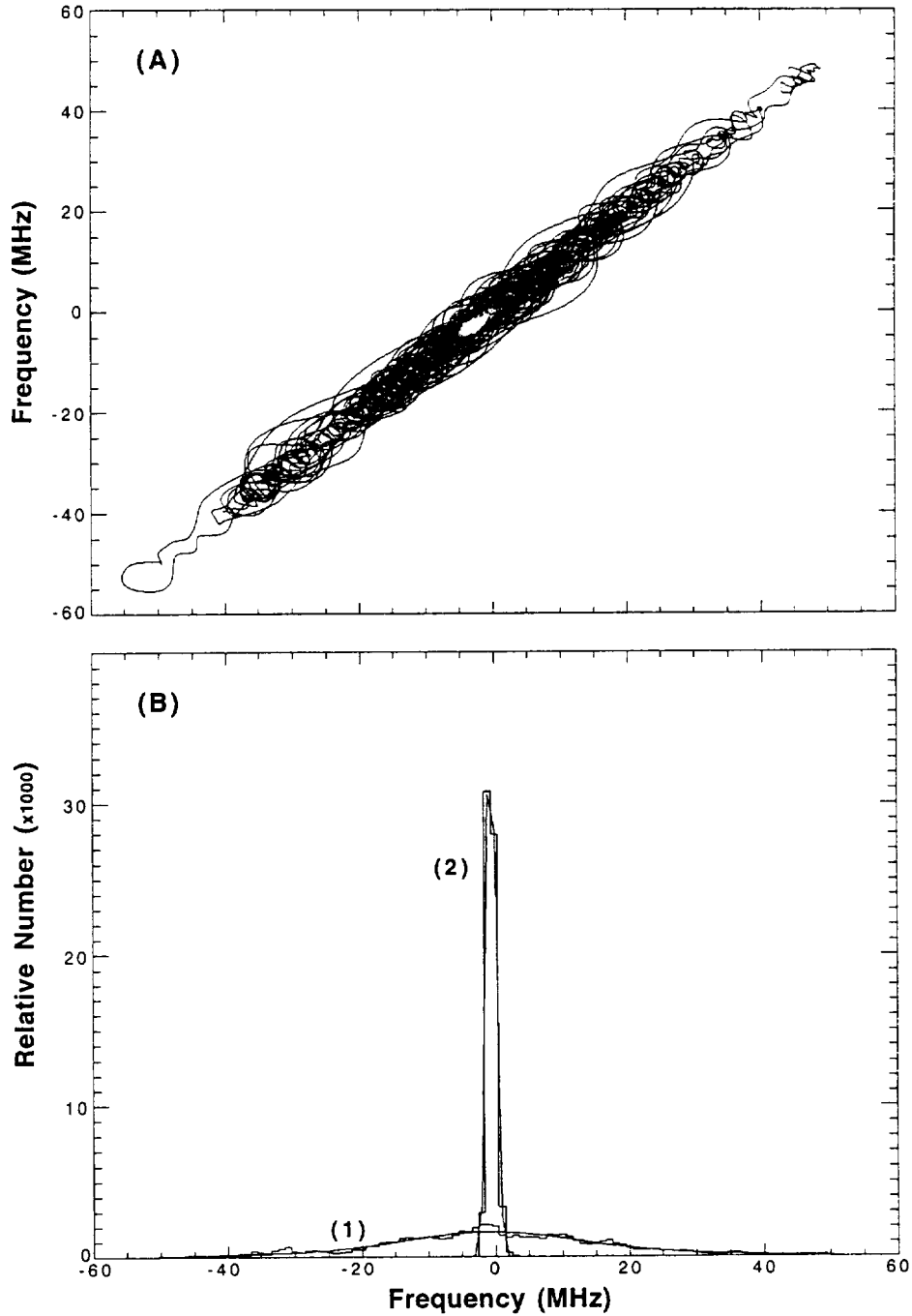


FIGURE 8 In (A) is a 2D time-delay phase plot of the chaotic uncontrolled (black) TDL and the OPF controlled (small white region at center) trajectories from the data in Figure 7. In (B) are histograms of the TDL trajectories in (A) (uncontrolled (1), controlled (2)) with bin widths of 1 MHz. Each histogram is then over-plotted with a Gaussian profile fit to the histogram data. For the uncontrolled emission the FWHM of the fitted Gaussian is 29.5 MHz, while for the controlled emission the FWHM is 1.45 MHz. This width of 1.45 MHz is an upper limit to the stabilized TDL frequency. The Ratio of the uncontrolled and controlled FWHM indicate an effective narrowing of the laser frequency output by a factor of 20.

immediate. There are numerous candidates for future OPF control, such as an optically pumped submillimeter laser that emits from 30 μm to 1 mm and whose output varies in a seemingly random fashion because of nonlinear feedback between the pump and lasant gas.

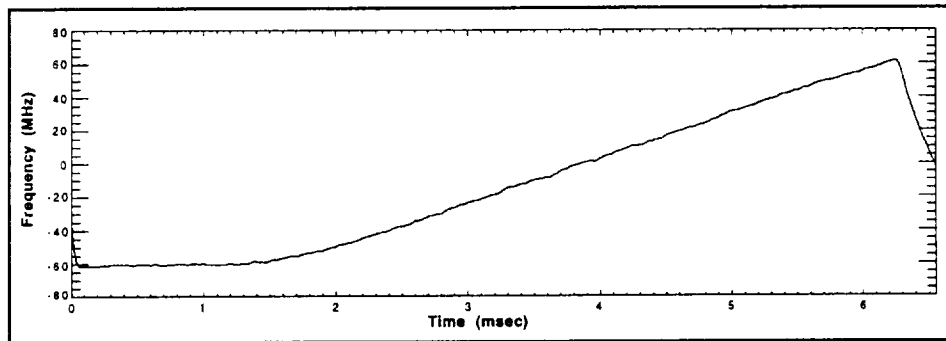


FIGURE 9 The center frequency of the TDL is scanned over a range of 120 MHz with the OPF controller activated. The ramp generator used was set for a 10 msec (100 Hz) scan, where the scan stays at the minimum value for 5 msec then increases for 5 msec before returning to the minimum value. At the right edge we can see where the OPF controller is retarding what would otherwise be a nearly vertical fall of the frequency back to the minimum value.

10. Acknowledgements

We wish to thank J. Lobell for designing the OPF electronics and G. Miller for putting it together. [They are in Code 692 of Goddard Space Flight Center (GSFC)]. M. Sirota and D. Reuter (Code 693) loaned us the diode laser for this experiment. We also wish to thank G. McGuire and P. Cummins of the UT Physics Department Electronics Shop for their assistance in the construction of version-2 of the OPF controller. This research is conducted under NASA cooperative agreement NCC 5-88 with the University of Tennessee, Knoxville, under the support of the GSFC Director's Discretionary Fund.

11. References

1. "Chaos in Communications," *Proceedings of SPIE 2038* (1993).
2. E. Ott, C. Grebogi, and J. A. Yorke, "Controlling Chaos", *Phys. Rev. Lett.* **64** (1990) 1196.
3. U. Dressler, G. Nitsche, *Phys. Rev. Lett* , **68**, 1, (1992); F. Romeiras, C. Grebogi, E. Ott, and W. P. Dayawansa, *Physica D* , **58**, 165, (1992); H. Wang and E. H. Abed, *Proceedings of IFAC Nonlinear Control Systems Symposium*, Bordeaux, (1992).
4. W. L. Ditto, S. N. Rauseo, and M. L. Spano, "Experimental Control of Chaos", *Phys. Rev. Lett.* **65** (1990) 3211.
5. J. Singer, Y.-Z. Wang, and H. H. Bau, "Controlling a Chaotic System", *Phys. Rev. Lett.* **66** (1991) 1123.

6. A. Garfinkel, M. L. Spano, W. L. Ditto, and J. N. Weiss, "Controlling Cardiac Chaos", *Science*, **257** (1992) 1230.
7. E. R. Hunt, "Stabilizing High-Period Orbits in a Chaotic System: The Diode Resonator", *Phys. Rev. Lett.* **67** (1991) 1953.
8. T. Takizawa, Y. Liu, and J. Ohtsubo, *IEEE Journal of Quantum Electronics*, **30** (1994) 334.
9. R. Roy, T. W. Murphy, Jr., T. D. Maier, Z. Gills, and E. R. Hunt, "Dynamic Control of a Chaotic Laser: Experimental Stabilization of a Globally Coupled System", *Phys. Rev. Lett.* **68** (1992) 1259.
10. Z. Gills, C. Iwata, R. Roy, I. B. Schwartz, and I. Triandaf, "Tracking unstable steady states: Extending the stability regime of a multimode laser system", *Phys. Rev. Lett.* **69** (1992) 3169.
11. D. E. Jennings, *J. Quant. Spectroscopy. Radiat. Transfer*, **40** (1988) 221.
12. D. E. Jennings, "Calibration of diode laser spectra using a confocal etalon", *Applied Optics*, **23**, No. 9 (1984) 1299.
13. G. Chin, L. R. Senesac, W. E. Blass, and J. J. Hillman, "Stabilizing Lead-Salt Diode Lasers: Understanding and Controlling Chaotic Frequency Emission", *Science*, **274** (1996) 1498.
14. J. P. Eckmann, S. O. Kamphorst, D. Ruelle, and S. Ciliberto, "Liapunov exponents from a time series", *Phys. Rev. A*. **34** (1986) 4971.
15. J. P. Eckmann, and D. Ruelle, "Ergodic theory of chaos and strange attractors", *Rev. Mod. Phys.* **57** (1985) 617.
16. M. Ding, C. Grebogi, E. Ott, T. Sauer, and J. A. Yorke, "Plateau onset of correlation dimension: When does it occur?", *Phys. Rev. Lett.* **70** (1993) 3872.
17. N. H. Packard, J. P. Crutchfield, J. D. Farmer, and R. S. Shaw, "Geometry from a Time Series", *Phys. Rev. Lett.* **45** (1980) 712.
18. T. C. Newell, P. M. Alsing, A. Gavrielides, and V. Kovanis, "Synchronization of a Chaotic Diode Resonator by Occasional Proportional Feedback", *Phys. Rev. Lett.* **72** (1994) 1647.
19. T. W. Carr, and I. B. Schwartz, *Phys. Rev. E* **51** (1995) 5109.